# Soft Matter

**REVIEW**

## Non-affine deformations in polymer hydrogels

Qi Wen,†[a] Anindita Basu,†[b] Paul A. Janmey[bc] and Arjun G. Yodh[b]

Most theories of soft matter elasticity assume that the local strain in a sample after deformation is identical everywhere and equal to the macroscopic strain, or equivalently that the deformation is affine. We discuss the elasticity of hydrogels of crosslinked polymers with special attention to affine and non-affine theories of elasticity. Experimental procedures to measure non-affine deformations are also described. Entropic theories, which account for gel elasticity based on stretching out individual polymer chains, predict affine deformations. In contrast, simulations of network deformation that result in bending of the stiff constituent filaments generally predict non-affine behavior. Results from experiments show significant non-affine deformation in hydrogels even when they are formed by flexible polymers for which bending would appear to be negligible compared to stretching. However, this finding is not necessarily an experimental proof of the non-affine model for elasticity. We emphasize the insights gained from experiments using confocal rheoscope and show that, in addition to filament bending, sample micro-inhomogeneity can be a significant alternative source of non-affine deformation.

## I. Introduction

Hydrogels are an important subclass of materials composed of three dimensional polymer networks swollen in water. A jelly is a hydrogel of polysaccharides;[1] contact lenses are hydrogels of silicone;[2] and cells in the human body are connected by hydrogels of collagen.[3] These hydrogels have mechanical properties common to both fluids and solids, *i.e.*, they are viscoelastic. The water in hydrogels makes them macroscopically incompressible and enables gels to "flow" like fluids; the polymer network structures provide mechanical support for the gels. It should not be surprising that the microscopic properties of polymers and the structure of polymer networks affect the elastic properties of

[a]Department of Physics, Worcester Polytechnic Institute, MA, USA.
[b]Department of Physics and Astronomy, University of Pennsylvania, PA, USA.
[c]Institute for Medicine and Engineering, University of Pennsylvania, PA, USA.
† Contributed equally to this work.
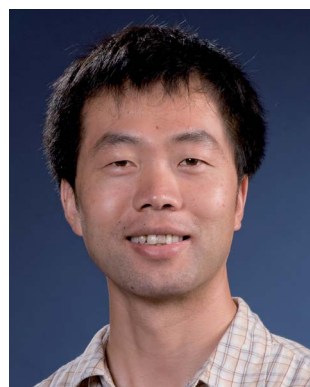
*Qi Wen is an assistant professor in the Physics Department of Worcester Polytechnic Institute. He received his PhD in Physics from Brown University in 2007 and worked as a post-doctoral researcher with Professor Paul A. Janmey and Professor Arjun G. Yodh at the University of Pennsylvania before joining Worcester Polytechnic Institute in 2011. His current research is focused on mechanics of biopolymer networks, with aims to understand the mechanical properties of tissue cells and their interaction with the extracellular materials.*

**Qi Wen**

*Anindita Basu is a doctoral candidate in Physics working under the supervision of Dr Arjun G. Yodh at the University of Pennsylvania. She is interested in the micro-structural behavior of bio-polymer and colloidal systems under macroscopic deformation. She received her B.S. in Physics and Computer Engineering from the University of Arkansas.*

**Anindita Basu**

hydrogels. Increased polymer concentration and crosslinker concentration, for example, can lead to enhancements in gel elasticity. The hydrophobicity of polymers can also be tuned to regulate hydrogel elasticity by changing pH[4] or temperature.[5] In fact, as a result of this tunable elasticity, hydrogels are widely applied in the food industry,[1] environment control,[6] medical instrumentation,[2,7] and medicine.[4,5,7] Thus, an understanding of the physical mechanisms affecting elasticity of hydrogels is useful.

The elastic behavior of most hydrogels of synthetic polymers such as polyethylene glycol (PEG) and polyacrylamide (PA) is similar to that of rubber-like materials. Their elasticity can be understood on the basis of the classic theory of rubber elasticity.[8] Hydrogels composed of biological polymers such as actin, collagen and fibrin, however, exhibit unique rheological properties such as strain-stiffening[9–12] and negative normal stress,[13–15] which are not observed in rubber-like materials. These unique mechanical properties may have biological significance, but a mechanistic understanding of these is beyond the scope of classic rubber elasticity theory.[10,16]

Ultimately, the elasticity of biopolymer gels originates from the resistance of polymers to stretching and bending deformations. Generally polymer stretching produces affine deformation of the gels, whereas polymer bending can give rise to non-affine deformation. Affine deformation implies a mechanical response with uniformly distributed strain, $\gamma$, i.e., the local microscopic strain is identical to the global macroscopic strain applied to the material. This idea is depicted by the schematic in Fig. 1, which shows a cross-section of polymer gel under shear. The grey circles along the vertical dashed line indicate the position of tracer beads entrapped in a gel under no external loading. When a shear force is applied on the top surface of the gel, the circles move as the gel deforms. If the gel were to deform affinely, the tracer beads would displace to new positions given by green circles, all of which lie along the oblique dashed line. However, if the
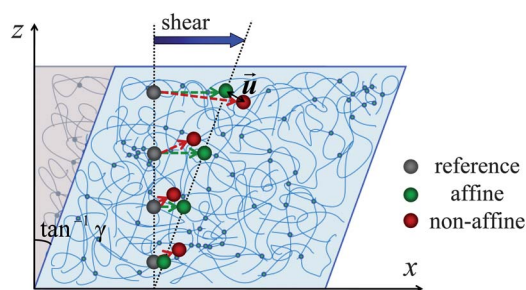


**Fig. 1** Illustration of affine and non-affine shear deformation of polymer gels with entrapped tracer beads. The non-affine deviation, $\vec{u}$ is defined as the difference between the real displacement and affine displacement of a tracer bead. This figure is adopted from ref 22.

deforms non-affinely, as real gels are wont to do, then the tracer beads displace to new positions in random, denoted by the red circles. The non-affine deviation, $\vec{u}$, is defined as the deviation of a tracer bead from its affine position, i.e., the distance between its respective red and green circles.

Two types of theoretical models account for the elasticity of biological polymer gels.[10,16–18] Both approaches are successful in predicting strain-stiffening and negative normal stress, i.e., the characteristic mechanical properties of biological gels. The first model is an affine model. Similar to the classical theory for rubber elasticity, it treats the biological filaments as entropic springs and assumes affine deformation, i.e., that strain is uniformly distributed in the polymer networks. According to this model, strain-stiffening of polymer networks originates from the nonlinear force extension curve of individual biopolymers.[10,16] The other theoretical approach is the so-called non-affine model in which enthalpic deformation of stiff filaments is the dominant contribution to elasticity. It predicts non-affine deformation due to bending and reorganization of the polymer filaments. Strain-stiffening in the non-affine model originates from network

*Paul Janmey received an A.B. degree from Oberlin College in 1976 and a PhD in Physical Chemistry from the University of Wisconsin in 1982, working in the lab of J.D. Ferry on fibrin polymerization. A post-doctoral fellowship in the Hematology Unit of Massachusetts General Hospital motivated application of methods of polymer physics to the cytoskeleton. Since then his lab has studied the viscoelastic properties of biopolymer networks and the regulation of cytoskeletal and extracellular matrix assembly. Current work is focused on the response of cells to the viscoelastic properties of their environment and on developing new soft biocompatible materials for tissue engineering and wound healing.*

**Paul A. Janmey**



*Arjun G. Yodh is the James M. Skinner Professor of Science at the University of Pennsylvania. He is Director of Penn's The Laboratory for Research on the Structure of Matter and its NSF-Materials Science Research & Engineering Center (NSF-MRSEC). His home department is Physics & Astronomy, and he holds a secondary appointment in the Department of Radiation Oncology in the Medical School. Yodh received his B.Sc. from Cornell University and his PhD from Harvard University. He joined the University of Pennsylvania faculty in 1988, following a two-year postdoctoral fellowship at AT&T Bell Laboratories. His current interests span fundamental and applied questions in soft matter physics, biomedical optics, and the optical sciences (see http://www.physics.upenn.edu/yodhlab/).*

**A. G. Yodh**

reorganization that leads to a transition from filament bending to filament stretching.[17,18] Experimental verification of these two models, however, is currently lacking.

One possible way to check the validity of these two types of theoretical models is to measure the non-affine deformation in biological gels. With reflectance and fluorescence confocal microscopes it is just now becoming possible to resolve individual polymer filaments in semi-flexible polymer networks.[19–21] Looking forward, by combining these microscopy techniques with rheometers or alternative loading devices, one can, in principle, generate an experimental apparatus required for probing non-affine deformations of individual polymers in semiflexible gels. Herein we will briefly review currently available theories on elasticity of hydrogels, experimental methods to detect non-affine deformations, and possible sources of non-affinity in polymer gels.

## II. Elasticity of hydrogels

The elasticity of hydrogels can be characterized by rheological measurements using commercially available rheometers. During a typical oscillatory measurement using a strain-controlled rheometer, the rheometer imposes an sinusoidal oscillatory shear strain on the sample of the form $\gamma = \gamma_0 sin(\omega t)$, and the shear stress, $\sigma$, required to generate such a deformation is measured. For a linear viscoelastic material, the resulting stress is also a sinusoidal function with a phase shift, $\phi$, i.e., $\sigma = \sigma_0 sin(\omega t + \phi)$. The material elasticity, the shear elastic modulus ($G'$), is calculated from the part of stress that is in phase with strain, i.e., $G' = \frac{\sigma_0}{\gamma_0} cos\phi$. The out-of-phase stress is used to calculate the viscous response, i.e., the shear loss modulus ($G''$): $G'' = \frac{\sigma_0}{\gamma_0} sin\phi$.

For crosslinked polymer networks, $G'$ is often much larger than $G''$, i.e., the elastic response of the gel dominates. For materials with nonlinear elasticity, stress does not increase linearly with strain, and therefore, the measured shear stress signal is not a simple sinusoidal function. Higher-order harmonics appear in the stress signal due to the nonlinear relationship between stress and strain. An alternative method to measure nonlinear elasticity is to impose a constant level of stress (or strain) and then superimpose a low-amplitude oscillatory deformation to obtain the so-called differential modulus, $K'(\gamma,\omega)$, of the material in its strained state.[11,12] For linear materials, $K'$ is independent of the degree of pre-stress but is a function of pre-stress or pre-strain for nonlinear materials. $K'(\gamma)$ is generally more strongly dependent on strain than is $G(\gamma)$, which integrates the viscoelastic response over the entire deformation cycle.

Most synthetic polymer networks, such as polyacrylamide, polyethylene glycol, and polyvinyl alcohol are composed of flexible polymer chains similar to the polymers in rubber. The elasticity of such synthetic polymer gels also share some characteristics of rubber elasticity. For example, to generate a sinusoidal shear strain, the required stress is also a sine function, as shown for a sample PA gel with bisacrylamide as crosslinker in Fig. 2(a)-(i). In this case, the $G'$ of the synthetic polymer gel is constant over a large range of strain. In Fig. 2(b), $G'$ of a sample PA gel is measured as a function of shear strain. $G'$ remains constant with increasing shear strain (data shown for

$\gamma = 0.01$–$0.4$); indeed, in this experiment, $G'$ remains constant as strain was increased from $\gamma = 0.01$ up to 1.2 before the test failed due to detachment of the gel from the rheometer plates.[22] At larger strains, beyond this linear elastic regime and beyond our experimental limit, nonlinear elasticity is expected in synthetic polymer gels similar to that observed in rubber-like materials at large deformations. $G'$ of synthetic polymer gels is also predicted to depend on crosslinker concentration, $c$, and temperature, $T$, i.e., $G' = ck_B T$.[23] $k_B$ is the Boltzmann constant. Measured dependences along these lines are shown in Fig. 2(c) and (d) where $G'$ for PA gels increases linearly with $c$ and $T$, respectively.

The $G'$ for biopolymer hydrogels, however, differs significantly from that of PA gels. As illustrated in Fig. 2(a)-(ii), the stress required to generate a relatively large amplitude sinusoidal strain in fibrin gel, the major component of blood clots, is no longer a sine function. Higher-order harmonics are seen in the stress response signal, indicating the nonlinear relationship between shear stress and shear strain. Instead of being a constant, the $G'$ of biological polymer gels often increases with increasing strain (Fig. 2(b)). For example, the elastic modulus of a fibrin gel can increase about 20 times from 45 Pa to 800 Pa, when the strain increases from $\gamma = 0.01$ to 0.8.[24] Such an increase in elastic modulus with increasing strain is referred to as strain-stiffening. Strain-stiffening is a universal behavior for crosslinked gels of semi-flexible biological polymers. Besides fibrin, gels made of F-actin, vimentin and collagen also exhibit strong strain-stiffening.[10] The strain-stiffening of biopolymer gels has potential biological significance; for example, they can protect tissues cells from extremely large deformations.[25] This nonlinear elasticity in biopolymer networks is better characterized by analyzing the stress-strain curves obtained by large amplitude oscillatory shear (LAOS) tests.[26]

Besides strain-stiffening, negative normal stresses are also observed in biopolymer gels composed of rodlike or semiflexible filaments.[13,14] When subject to shear deformation, these biopolymer gels tend to pull the shearing surfaces toward each other. This inward pulling force is referred to as the negative normal stress.[13] In contrast, a gel formed by flexible polymer chains such as polyacrylamide has negligible normal stress at small deformation. At large strain, PA gels, like simple synthetic elastomers, generates positive normal stress, which tends to push the shearing surfaces away from each other. The magnitude of positive normal stress in PA gels is much smaller than the shear stress.[13] In contrast, the magnitude of negative normal stress in biopolymer gels is comparable to the shear stress and increases nonlinearly with increasing strain.[13,14] Under certain conditions, the magnitude of negative normal stress may even be larger than the magnitude of the applied shear stress.[14,15,27]

There is also significant influence of crosslinks on the macroscopic mechanical properties of hydrogels. Broadly, gels can have two types of crosslinks. Gels can be crosslinked physically wherein polymer chains are held together through attractive forces arising from chain entanglements, electrostatics, or van der Waals attractions;[28,29] or gels can be chemically crosslinked (e.g., polyacrylamide, polystyrene, etc.) wherein crosslinks are covalently bonded to the polymer chains.[28,30,33] Physically crosslinked gels are generally weaker than chemically crosslinked gels, are more likely to rearrange under shear, and often tend to yield under increasing strain.[28,29] Chemically crosslinked gels
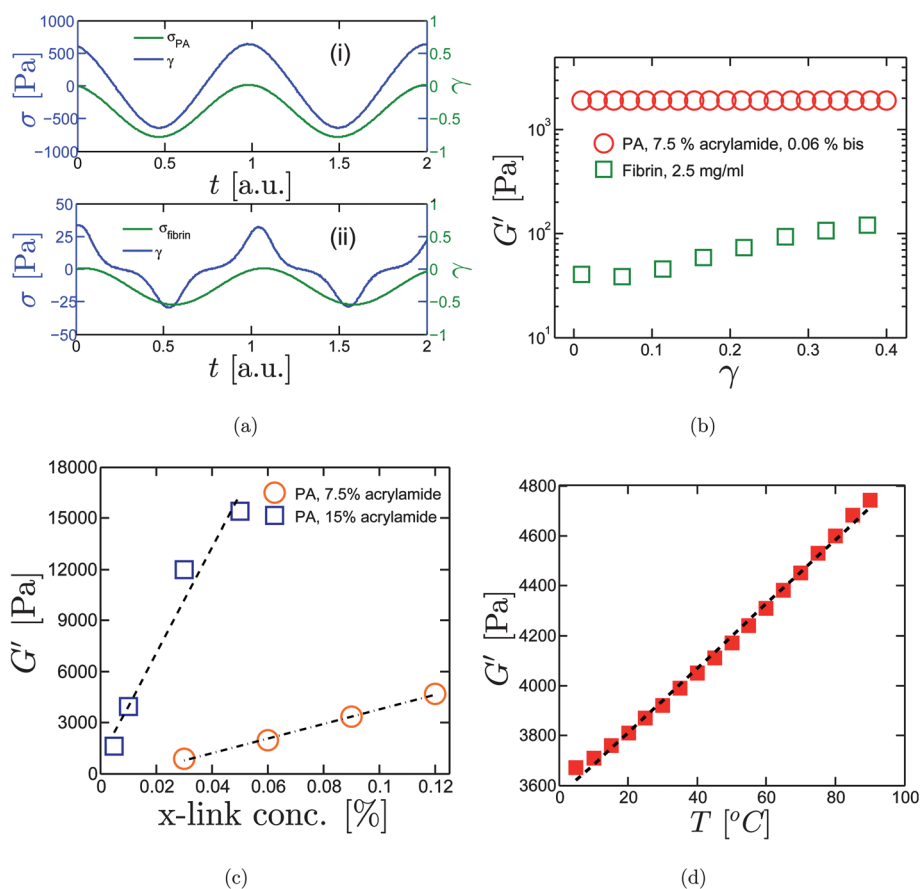
**Fig. 2** Mechanical properties of hydrogels. (a) Stress *vs.* strain of (i) PA and (ii) fibrin gels. (b) Elastic modulus *vs.* strain of PA gels, fibrin and collagen gels. (c) $G'$ *vs.* crosslink concentration in PA gels with 7.5% (w/v) and 12% (w/v) acrylamide. (d) $G'$ as a function of temperature in a crosslinked PA gel (7.5% acrylamide and 0.09% bis).

have comparatively higher moduli, are composed of individual polymer filaments that have largely lost their distinguishability, and deform by bending or stretching out polymer filament sections between static crosslink junctions, rather than by release or movement of crosslinks.[31]

The crosslink situation in bio-polymer gels is even more complex. Gels that yield irreversibly are considered to have chemical crosslinks, be they covalently bonded or formed by branching filaments. In addition, bio-polymer filaments may be composed of bundles of smaller fibril units that are laterally stacked[33,47] and held together by multivalent counterions.[32,47] These electrostatic forces, while being sufficiently strong to give the polymer filaments mechanical rigidity, permit the fibrils to slide against each other under external deformation. Such fibril bundles tend to align in the direction of loading, often irreversibly under sufficiently high strains.

## III. Affine model of elasticity

Affine deformation is one of the fundamental assumptions in the classical rubber elasticity theories. Following this assumption, each polymer strand is stretched to a strain which is the same as the strain applied over the whole sample; thus the network elasticity originates from the resistance of individual polymers to stretching.[16,23] With the affine assumption, the elasticity of

rubber is derived from the entropic elasticity of each individual polymer.[23] Using the affine assumption that each crosslinker displaces affinely under external load, phantom network models by Flory[34] and Guth[35] derive network elasticity from the decrease in network configurational entropy.

Using the affine assumption, both linear elasticity and nonlinear strain-stiffening in hydrogels can be understood on the single molecule level as a direct consequence of the mechanical response of worm-like-chains (WLC).[10,16,36] Within this approach, the end-to-end distance of the WLC, *i.e.*, $R$, in the crosslinked network is set to be the average distance between crosslinkers, $L_c$; $L$ is the average contour length of polymer segments between two neighboring crosslinkers.[16,36] Thermal agitations lead to transverse undulations, which cause the distance between the ends of a WLC to be smaller than the polymer length, *i.e.*, $R < L$.[10,16,23] Stretching a WLC, in other words, increasing $R$, is equivalent to pulling out the extra contour length and leads to a decrease in conformational entropy of the polymer.[10,16,23] The force to keep the end-to-end distance of a WLC at $R$ is[37]

$$F = \frac{k_B T}{l_p}\left[\frac{1}{4(1 - R/L)^2} - \frac{1}{4} + R/L\right], \qquad (1)$$

where $l_p$ is the persistence length quantifying the stiffness of a polymer. When $l_p \ll L$, a polymer is flexible; when $l_p \gg L$,

a polymer is stiff. Most biological polymers are semiflexible with $l_p$  $L$. The relationship between $l_p$ and $L$ also determines mean-square end-to-end distance of a *free* WLC as:

$$\langle R^2 \rangle = 2l_p L[1 \quad l_p/L(1 \quad e^{L/l_p})], \quad (2)$$

When a network deforms affinely, each polymer is stretched to the same amount so that the end-to-end distance increases by an amount $\delta R = \gamma L_c$. The stress-strain relation and hence the differential elastic modulus $K'$ of the gel, is then determined by the force-extension of a single WLC as

$$K' = \frac{d\sigma}{d\gamma} \quad \frac{dF}{dR}. \quad (3)$$

For a flexible polymer, $\sqrt{\langle R^2 \rangle} = 2l_p L$. The end-to-end distance $R$, and hence $L_c$, are much smaller than the contour length, $L$, of the WLC due to the small $l_p$. Therefore, the stretching deformation $\delta R = \gamma L_c$ is much smaller than $L$ for strains up to a few hundred percent, and eqn (1) gives $F \propto R$, *i.e.*, the force required to stretch a flexible WLC depends linearly on the extension for a very wide range of strain. According to eqn (3), the linear part of the force-extension of single WLC gives rise to the linear elasticity of flexible polymer networks, *i.e.* $K' = d\sigma/d\gamma$ is a constant.

For semi-flexible polymers, $R$ is comparable to the polymer length, because $l_p$ and $L$ are comparable. Thus, $F$ is no longer a linear function of $R$ but diverges as $1/(1 \quad R/L)^2$. The relationship between $F$ and $R$ for semiflexible polymers has been determined experimentally as $dF/dR \propto F^{3/2}$.[37] This nonlinear force extension results in the strain-stiffening of semiflexible polymer gels.[10,16] Following eqn (3), the affine model predicts a nonlinear elasticity as $K' \propto \sigma^{3/2}$. This strain dependence of elastic modulus is confirmed by experiments on actin gels.[11] Similar strain-stiffening behavior has also been observed in gels of intermediate filaments, and fibrin protofibrils.[10]

In addition to the entropic nonlinear elasticity of thermally undulating polymers, effects such as mechanical stretching and compression of stiff polymer segments between crosslinkers can also contribute to the elasticity of semiflexible and stiff polymer networks.[36] Such an affine mechanical stretching model can account for the elasticity of gels made of actin bundles and thick fibrin fibers.[11] The stretched filaments oriented away from the direction of shear produce a downward force, which gives rise to negative normal stress in the biopolymer gels.[13]

## IV. Non-affine deformation and gel elasticity

In spite of its successes in capturing the essence of both linear elasticity of flexible polymer gels and strain-stiffening of semi-flexible polymer gels, the affine assumption is simplistic. In affine models, for example, interactions between polymers are ignored so that each polymer deforms independently without affecting their neighbors. Such a deformation can only occur under ideal conditions.[38] In reality, all material deformations are expected to be non-affine on some length-scale. Indeed, non-affine deformation has been observed in many materials, including foams, synthetic polymer gels, and biological materials.[22,24,36,38–41]

### A. Origins of non-affine deformation

Many factors lead to non-affine deformation in hydrogels. Inhomogeneities can play a major role in the degree of non-affinity in polymer gels. Didonna and Lubensky demonstrated theoretically[38] that variations in local elasticity lead to spatially correlated non-affine deformation in random, elastic media. The magnitude of this non-affinity was predicted to be proportional to the variance in local elastic moduli.[38] Experiments[22] indicate that network inhomogeneities formed during sample preparation are a major source of non-affinity in flexible polymer gels like PA gels. Fig. 3 is a schematic of some common network imperfections that can lead to inhomogeneities flexible polymer gels: (a) closed loops of polymer chain, wherein a crosslinking unit is attached to the ends of the same polymer chain instead of connecting two chains together, (b) dangling polymer chain ends, (c) crosslinks reacting among themselves instead of with polymer chains, and (d) polymer chain entanglements that tend to slip under external loading.[42] Inhomogeneity in crosslink and polymer concentrations may also occur during polymerization. The size of the inhomogeneities can range anywhere from tens of nanometers to a micrometer[43] which determines the non-affinity length-scale, *i.e.*, the length-scale above which the gels deform affinely.

Inhomogeneities are not restricted to flexible polymer gels only. Non-affine deformation of collagen networks in porcine skin under compression is also attributed to the presence of inhomogeneities. Deformations larger than the average size of these inhomogeneities are seen to be essentially affine.[44]

Experimentally, observed deformations in a polymer gel under external load can be affine or non-affine depending on the length-scale examined.[45] Different polymer gel classes have different "important" length-scales, *viz.*, persistence length of the constituent polymers, end-to-end length of filaments, mesh-size, *etc.* For an isotropic, crosslinked polymer network, there is an intrinsic non-affine length-scale, $\lambda = l_c(l_c/l_b)^{1/3}$,[36,46] depending on gel morphology. Here $l_c$ is the length of polymer chain between crosslinks, $l_b = \sqrt{\kappa/\mu}$ is a measure of the natural bending length of the filaments, and $\kappa$ and $\mu$ are the bending and stretching modulus of the polymer chain, respectively. When modeling
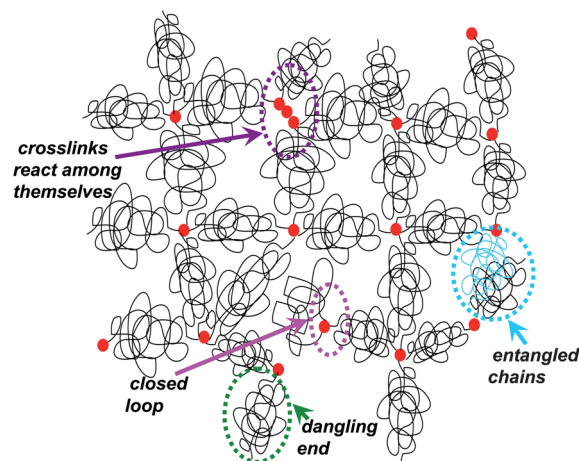


**Fig. 3** Inhomogeneities in crosslinked polymer gels.

a filament as an elastic cylinder, $l_b$ is approximately the filament radius. The affinity/non-affinity of network deformation depends on the relationship between filament length $L$ and $\lambda$. At large $l/\lambda$ (*i.e.*, $l/\lambda > 1$), when the network is highly crosslinked, network deformation is affine. Conversely, for a loosely crosslinked network, $l/\lambda$ is small (*i.e.*, $l/\lambda < 1$) and deformation is non-affine. Increasing either the polymer chain density or the crosslink concentration can effectively decrease $l_c$, thereby decreasing $\lambda$[36] and causing the network deformation to transit from a bending dominated non-affine regime to a stretching dominated affine regime. Also, biopolymer filaments can bundle together under certain conditions, *e.g.*, pH[47] and shear.[14] Formation of bundles changes the value of $l_b$, and hence, the mode of deformation in the locality of the bundles. Of course, a polymer network with filament bundles randomly interspersed must be inhomogeneous on the length-scale of the filament bundles. The non-affinity measure is also affected by the amount of strain applied: under extensional forces, non-affinity has been measured to increase with increasing strain,[48] and under shear, non-affinity decreases as strain increases.[24] As examples of such non-affinity, Fig. 4(a) plots the mean square of non-affine deviation, $\vec{u}$ from affine displacement position (see Fig. 1), *i.e.*, $\langle|\vec{u}|^2\rangle$ as a function of applied strain, $\gamma$ for polymer gel samples of PA (7.5% acrylamide, 0.03% bis)[22] and fibrin (2.5 mg mL$^{-1}$, pH = 7.4).[24] $l_p$ is 3 Å in PA gels and 500 nm in fibrin gels shown here. The measured non-affinity increases with the increasing stiffness of the constituent polymer filaments.

Simulations of 2D athermal networks of rigid rods[17] mimic gels consisting of stiff polymer filaments. Under shear, such a system exhibits filament-bending at low strains, and network rearrangements under high strains, both causing non-affine deformations. Network rearrangements were observed in collagenous tissue, albeit under uniaxial extension,[48] especially when loaded perpendicular to the natural alignment of collagen fibers; here, the stiff fibers reoriented *en masse* to align with the direction of extension. Such non-affine bending and rearrangement in (non-covalently bonded) stiff collagen filaments that form the underlying substrate have been shown to have profound effects on the shape, proliferation and motility of mammalian cells.[49]

There are yet other sources of non-affine deformation. The effect of network connectivity on elasticity and non-affinity has been investigated by Broedersz, *et al.*[50] using a lattice-based model of stiff rods with variable connectivity. In addition, loading history,[48] pre-shear conditions,[51] and gelation kinetics,[22] also have influence on gel morphology and hence non-affinity measures.

## B. Gel elasticity due to non-affine deformation

Over the years, there has been continued effort in determining the consequence of non-affinity in polymer gels. Rubinstein proposed a model based on microscopic non-affine deformations to account for the nonlinear elasticity of polymer networks. In an
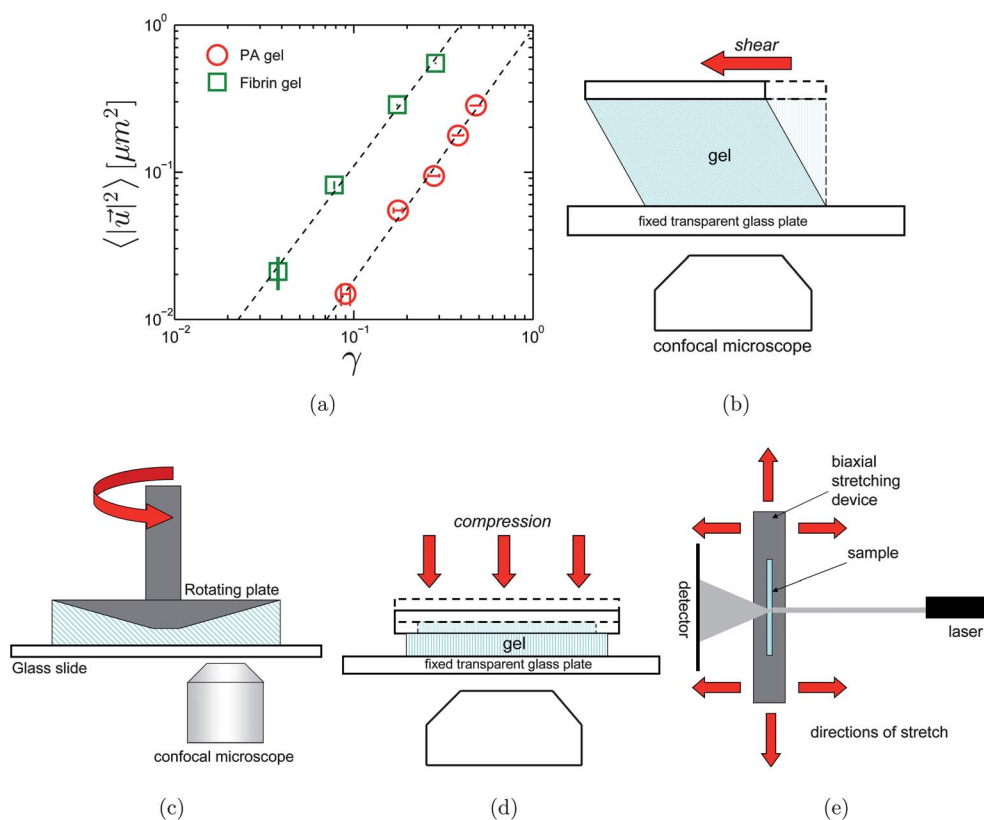


**Fig. 4** (a) Mean square non-affine deviation, $\langle|\vec{u}|^2\rangle$ as a function of applied strain, $\gamma$ in PA gel (7.5% acrylamide, 0.03% bisacrylamide) and fibrin gel (2.5 mg mL$^{-1}$ fibrinogen) samples. Illustrations of (b) optical shear cell, (c) confocal rheoscope, (d) video microscopy setup on gel under compression, and (e) light scattering on gel under biaxial stretching.

entangled network, each polymer is confined within a tube-like region due to the steric interaction with its neighbors.[52] Within the tube, the polymer deforms non-affinely by changing its conformation. The effect of steric interaction between neighboring polymers is then considered as the confining potential imposed by such a tube. Besides the conformational entropy, this confinement also alters the effective elasticity of a polymer.[45,53] Rubinstein and Panyukov found that the size of the confining tube, and hence the confining potential changes non-affinely with external deformation.[45] As a result of such a non-affinely varying confining potential, Rubinstein, *et al.*[45] demonstrated that the microscopic non-affine deformation leads to a nonlinear stress-strain relation similar to the empirical Mooney–Rivlin relation for flexible polymer networks at large deformations.

For semi-flexible and stiff polymer networks, in addition to the confining tubes, the finite stiffness of polymers should be considered. In these networks, such as a highly crosslinked isotropic network of actin, a single polymer of length, $l$, can be crosslinked multiple times, say $n$, such that the average length of the polymer segments between crosslinkers is $L_c = l/n$. The deformation of segments that belong to a single actin filament should be correlated due to the bending rigidity of the filament. The ratio of effective spring constant for filament-stretching to the spring constant for filament-bending, which is proportional to $l_p/L_c$, determines the details of network deformation.[36,54] When $L_c \gg l_p$, as in a sparsely crosslinked network, it is much easier to stretch a filament than to bend it. In contrast, if $L_c \quad l_p$, as in stiff filament networks or highly crosslinked semiflexible polymer networks, stretching a filament is much harder than bending one. Filament bending causes "floppy modes" in the network,[54] which give rise to the network elasticity and the non-affine network deformation.[54,55] The network elasticity due to bending deformations of individual polymers is inherently linear.[11,56] Rather than the nonlinear stretching of filaments, geometric effects such as the transition from filament bending/buckling dominated non-affine network deformation to a stretching dominated affine deformation give rise to the strain-stiffening.[17,18,57] For sufficiently large strains, however, filament-buckling may even lead to a *decrease* in elasticity of actin gels;[58] this decrease is reversible in that the filaments will unbuckle when the strain is released. When $L_c$ and $l_p$ are comparable, both affine filament stretching and non-affine filament bending contribute to network deformations.[46,55]

Non-affine deformation models also predict negative normal stress in biopolymer gels from filament stretching and buckling.[15,18] As strain increases the magnitude of negative normal stress may become larger than the shear stress due to the buckling of filaments at large strains.[14,15,27]

## V. Experiments to detect non-affine deformations

An experimental setup ideal for investigating non-affinity in polymer gels consists of a mechanical loading apparatus coupled to an imaging device that can visualize the gel under external load. Although most existing theories consider the problem of non-affinity under shear, the non-affinity question is pertinent for a variety of loading techniques, *e.g.*, extensional,[48] compressive[44] or shear.[22,24,51] Piezo-electric micromanipulators

are becoming increasingly popular for loading purposes, but any vice-like loading device is sufficient for applying uniaxial and biaxial forces. Rheometers are an excellent choice for applying tangential loads while also permitting rigorous characterization of viscoelastic properties of polymer hydrogels.[22,24] Light-scattering techniques[48] can be useful to probe ensemble-averaged behavior of gels under external loading. Also, confocal[22,51,59] and polarized light microscopes[60] are popular choices for quantifying non-affinity at sub-micron length-scales.

### A. Optical shear cell

An optical shear cell along with a confocal microscope was used by Liu, *et al.*[51] to measure non-affinity in F-actin gels with scruin crosslinks. The shear cell consisted of a fixed upper plate and a moveable lower plate, the lower plate being a cover-slip controlled by a piezo-electric actuator for shear strains up to $\gamma = 0.3$ and by a micrometer for larger strains, as illustrated in Fig. 4(b). The two plates were separated by 100 μm. Crosslinker concentration was varied by changing actin (monomer) to scruin (crosslink) ratio. The effect of polymer filament length on non-affinity was investigated by the use of the capping protein gelsolin. Macro-rheology and micro-rheology measurements were used to characterize the mechanical characteristics of the crosslinked polymer gels.

0.5 μm polystyrene (PS) tracer beads were embedded in the actin gels and tracked under shear using a confocal microscope. One advantage of using tracer beads to probe non-affinity is the ease with which one can study the problem at different length-scales. The size of the tracer particles determine the non-affinity length-scale investigated. There is an implicit assumption of course, that the deformations of the tracer particles reflect the non-affine deformation of the gels under study. To ensure that is indeed the case, one must take the coupling efficiency of the tracer particles with the polymer networks into consideration. There may be incomplete coupling of the tracer beads with the network, and the network morphology immediately surrounding the tracer beads may also be affected by the presence of the tracer beads.[61,62]

Two measures of non-affinity were used in this study.[51] The first is a two-point non-affinity measure which is length-scale dependent:

$$N(r) = \langle r^2 \Delta\theta^2 \rangle_r / \gamma^2, \tag{4}$$

where $r$ is the distance between a tracer-bead pair, $\Delta\theta$ is the angle of deviation between them under shear, and $\gamma$ is the applied strain. Measurements corroborate the physical picture supposed in the paper that, for a weakly crosslinked gel, $N(r) \approx r^{0.3}$, is approximately independent of the bead separation. For a densely crosslinked gel, however, there is a weak power-law dependence of $r$ on $N$: $N(r) \approx r^{0.6}$, for the gel with the highest concentration of crosslinks. Overall, the magnitude of $N(r)$ decreases as cross-link density is increased. This is due to the decrease in network elasticity, which results in decreased energy-cost for local strain fluctuations.

The second non-affinity measure, $S$ is a scalar quantity that is useful in comparing non-affinity in polymer gels with different degrees of crosslinking:

$$S = \langle \Delta \vec{r} \cdot \Delta \vec{r} \rangle / \gamma^2. \tag{5}$$

Here, $\Delta \vec{r}$ is the deviation of a tracer bead from its affine displacement position under shear.

By systematically varying the filament length, $l$, and cross-linker density, Liu, et al. found that the non-affinity, measured using both $N(r)$ and $S$, decreases as $l/\lambda$ increases. At large $l/\lambda$, $S \approx 3\ \mu m^2$, and strain-stiffening is observed in the actin networks. When $l/\lambda < 4$, $S$ increases to approximately $10\ \mu m^2$, and there is no strain-stiffening in the network. Low $S$ values suggest that network deformation is dominated by affine stretching of actin filaments, and that the strain-stiffening has an entropic origin. The high measures of $S$ are interpreted as the result of non-affine network deformation due to filament bending. Taken together, a transition from affine to non-affine deformation is observed as $l/\lambda$ is decreased in this set of experiments, consistent with predictions of Head, et al.[36]

Liu, et al. were also able to characterize the mechanical properties of soft actin gels using micro-rheology measurements, which derives the viscoelasticity of soft materials from the thermal motion of tracer beads. To acquire meaningful micro-rheology data, the material has to be soft enough so that thermal motion of tracer beads are detectable. This thermal motion can also lead to fluctuations in the tracer beads around its affine deformation location and thus contribute to the measured non-affine network deformation. There is no such comparison of the magnitude of thermal motion with the non-affine deformations in actin networks, however.

## B. Rheoscope

A rheoscope interfaces a rheometer with an inverted microscope that enables visualization of the deformation resulting from the external stress applied by the rheometer. Such a setup was used by Wen, et al.[24] to quantify shear deformation in semi-flexible polymer gels by measuring the displacements of fluorescently labeled micron-sized PS tracer beads entrapped in 2.5 mg mL$^{-1}$ fibrin gels at pH 7.4. The fibrin is polymerized from fibrinogen, in the presence of thrombin, both fibrinogen and thrombin having been extracted from blood plasma. At this concentration and pH, fibrin gels consist of semi-flexible bundles ($l_p \approx 500$ nm) of fibrin filaments which form an isotropic 3D network. The mesh-size, $\xi$ of the network is on the order of 200 nm, which means that the gel forms a semi-flexible polymer network, since $l_p/\xi \approx 1$. Accordingly, the gels exhibit dramatic strain-stiffening behavior as well as significant negative normal stresses, both characteristic of semi-flexible polymer gels. Optically transparent fibrin gels are polymerized in the rheometer in situ, such that gels can establish good contact with the rheometer plates, minimizing slippage. Macroscopic rheological behavior of the gels is characterized; fibrin gels exhibit marked strain-stiffening and negative normal stresses that decreases quadratically with strain.

A rough schematic of the experimental set-up is given in Fig. 4(c). Under fluorescence illumination, the location of the tracer beads in fibrin gel can be accurately determined in the $xy$ plane with sub-pixel accuracy from the well-defined spatial maxima of their point-spread functions. The $z$ location of the tracer beads are mapped by mounting the microscope objective

on a piezo-electric actuator. A unitless non-affine parameter, $\mathscr{S}$, is defined as

$$\mathscr{S} = \frac{1}{N} \sqrt{\sum_{i=1}^{N} \left( \frac{d_i - z_i \gamma}{z_i \gamma} \right)^2}, \tag{6}$$

where $N$ is the number of tracer beads tracked, $d_i$ is the displacement of the i-th tracer-bead under an external strain $\gamma$, and $z_i$ is the $z$-distance of the i-th bead from the fixed lower plate. The $\mathscr{S}$ defined here is the ratio between the non-affine to affine displacements, averaged over all tracked tracer beads.

It is seen that the measured non-affinity is low ($\mathscr{S} < 0.1$) and decreases further with increasing strain. Also noteworthy is the fact that the strain at which non-affinity starts to decrease coincides with the onset of strain-stiffening behavior in these gels. The asymmetric force-elongation behavior in semi-flexible gels, which result from the imbalance of bending-to-stretching forces in the filaments, was considered[24] to be the origin of negative normal stresses as well as strain-stiffening in crosslinked semi-flexible polymer networks.[10,13,14] However, due to the poor spatial resolution of displacements along the $z$-axis, these measurements most likely underestimate the non-affinity in fibrin gel deformation.

## C. Confocal rheoscope

A confocal rheoscope couples a confocal microscope with a commercial rheometer, as shown in Fig. 4(c), which together, can apply stress to the sample confined between the rheometer plates and detect the resulting deformation in the sample.[22,59,63] Such a setup was used by Basu, et al.[22] to study non-affine shear deformation in polyacrylamide (PA) gels. PA gels consist of flexible chains of poly(acrylamide) that are crosslinked with bisacrylamide. The gels were embedded with $\approx 1\ \mu m$ fluorescent PS tracer beads, the centroids of which were tracked before and under shear. Displacements of the tracer beads were regarded as a measure of the local deformations in PA gels. Affine displacements of beads are calculated from the bead locations and the applied strain; the non-affine deviation, $\vec{u}$, (see Fig. 1) is calculated as the difference between the measured bead displacement and the calculated affine displacement. The main findings were that the mean-square non-affine deviation, $\langle |\vec{u}|^2 \rangle$, of tracer particles in the flexible polymer gels scales linearly with the square of the applied strain, $\gamma$, viz.,

$$\mathscr{A} \equiv \langle |\vec{u}|^2 \rangle \propto \gamma^2. \tag{7}$$

This result was predicted by Didonna, et al.[38] for random elastic solids. Contrary to theoretical predictions, however, there was no dependence of the measured non-affinity on either polymer chain density or crosslinker concentrations. Rather, the non-affinity measures were dominated by the spatial inhomogeneities inherent in PA gels.[43] PA gels are widely used as model flexible polymer gels that are optically clear and spatially uniform in macroscopic length-scales, but microscopic inhomogeneities $\approx 200$ nm are posited to cause non-affine shear deformations. Reaction kinetics, which can influence the size of the inhomogeneities formed during sample preparation, are seen to affect non-affinity measures.[22] The structural inhomogeneities

results in heterogeneities in microscopic elasticity in PA gels. Following the lines of Didonna's theory,[38] the magnitude of fluctuations in microscopic elasticity is estimated to be as much as 7 times larger than the macroscopic elasticity.[22] Note that $\mathscr{A}$ is related to the non-affinity measure, $S$ defined in eqn (5) as $S = \mathscr{A}/\gamma^2$.

Compared to an optical shear cell setup, the confocal rheoscope has the advantage of simultaneously performing rheological measurements and confocal microscopy. Using such a setup, Schmoller, et al.[63] observed that cyclic shear results in structural changes in the bundled actin networks, which give rise to strain-hardening of semi-flexible polymer gels.

## D. Light microscopy on compressed gels

Non-affine deformation in porcine skin under compression was measured by Hepworth, et al.[44] using a combination of micromanipulation device and microscopy. Porcine skin can be viewed roughly as a network of collagen fibers interspersed in a softer protein matrix. In this paper, in vitro porcine skin was subjected to uniaxial compression that allowed unhindered lateral expansion (Fig. 4(d)). The reorientation process of the fibers in the skin tissue was studied using an optical microscope. The angle of reorientation of the tissue fibers was compared using an affine deformation model. The experiment found that skin tissues underwent constant-volume compression up to 15% compression. For compressions greater than 15%, the amount of lateral expansion under compression was noted to depend on the initial fiber orientation in the samples. At micro-meter length-scales, the fiber reorientations were non-affine with large variations in reorientation angles. It was noted that the tissue samples were composed of heterogeneous components, viz., a network of thick collagen fiber bundles was interspersed in a softer, fluid-filled matrix of proteins with differential deformation under load that lead to non-affine deformation. However, the samples were more or less uniform over millimeter length-scales, meaning that deformations were approximately affine at such length-scales.

Huyghe, et al.[64] investigated bovine intervertibral discs under compression, using confocal microscopy. Intervertibral discs consist of fluid-filled extra-cellular matrix (ECM) that, in turn, is composed of collagen fibers and proteoglycans (PG). Charge carried by proteoglycans lead to a difference in osmotic pressure between the collagenous tissue and the surrounding fluid, causing the tissue to swell. (Normally, this swelling is constrained by vertibral discs.) The intervertibral discs were thinly sliced, fluorescently labeled, compressed, and studied using digital image correlation techniques while under compression. Dead cells trapped in the ECM were also labelled. Each sample was placed in a salt bath at physiological osmotic conditions, covered by a dialysis membrane, and then filled with a solution of polyethylene glycol on the top. The compression force was a result of the osmotic pressure difference between the sample and PEG solution; the resultant pressure on the sample was varied by varying PEG concentration. Measurements show that tissue deformation under external load is highly non-affine, with strain fields around discontinuities like entrapped dead cells, being particularly inhomogeneous. In addition, significant normal strains were detected between collagen fibrils under external loading.

## E. Non-affine measurements on gels under uniaxial and biaxial stretching

A custom-built biaxial stretching apparatus coupled with a Small Angle Light Scattering (SALS) set-up was used by Gilbert, et al.[48] to quantify non-affine deformation under uniaxial and biaxial stretching, as shown in Fig. 4(e). The set-up was used to study 100 μm-thick samples of porcine small intestinal submucosa (SIS). SIS consist of collagen fiber scaffolds that can be useful for tissue remodeling.[65] Unlike the isotropic filament networks that have been considered so far, collagen fibers in SIS have a preferred direction (PD) of orientation.[39] Samples were strained both along the preferred orientation direction and perpendicular to it. The stretching device consisted of a system of pulleys that were rotated using stepper motors. An unpolarized HeNe laser beam was incident on the strained sample; the light scattered off it was detected using a CCD camera. The angular distribution of the strained collagen fibers was measured from the light scattering pattern. The correlation, $r^2$ to the affine model prediction was defined as:

$$r^2 = 1 - \frac{MSE}{var R_D(\theta)}, \tag{8}$$

where $MSE$ is the mean square deviation in the experimentally measured statistical fiber distribution, $R_D(\theta)$, from the affine prediction, and var is variance. Results indicate that biaxial stretching is affine with a high index of correlation ($r^2 > 0.98$). Under uniaxial stretch, however, fiber reorientation is significantly less than that predicted by the affine deformation model. Along PD, $r^2$ progressively decreased to 0.67 with increasing strain. When stretched perpendicular to PD, fibers reoriented such that the PD changed by as much as 70° to the initial PD to align with the direction of loading, with $r^2$ as low as 0.3.

Thomopoulos, et al.[66] studied the effect of collagen gel polymerization under uniaxial and biaxial loading constraints on cardiac fibroblast-populated collagen I gels. Titanium oxide dots embedded in the gels were tracked under deformation, using confocal reflectance microscopy. Gels synthesized under uniaxial constraints showed high degrees of anisotropies, both structural (collagen fibers aligned in the constrained direction) and mechanical (strains in the constrained direction were much lower than strain in the unconstrained direction). The high degree of mechanical anisotropy however, was incommensurate with the degree of structural anisotropy, and could not be not sufficiently explained by theoretical models that can adequately relate gel structure with mechanical behavior in unconstrained gels. Gels synthesized under biaxial loading constraints were found to be both structurally and mechanically isotropic.

Direct imaging of collagen gels using confocal microscopy with[59,67] and without[21] external load is useful to study mechanical properties of semi-flexible polymer networks. Collagen gels are a popular choice for this purpose – its fibers have high albedo which allows confocal reflectance microscopy[21,67] of the gels, bypassing the need of fluorescent labelling. Reflectance confocal microscopy of collagen gels under stretching was used by Vader, et al.[67] to study alignment of the fibers in collagen gels. Their findings indicate strong fiber alignment with growing strain in both crosslinked and uncrosslinked collagen gels. While such alignment is irreversible in uncrosslinked gels, it is completely

reversible in crosslinked ones. This indicates that network rearrangements are not irreversible or plastic deformations; rather high correlation between fiber alignment and strain-stiffening in the gels point towards network rearrangements as being inherent to non-linear elasticity.

## VI. Conclusions

Recently, numerous theoretical and experimental studies have addressed the origin of elasticity of hydrogels, in particular the strain-stiffening of semiflexible biopolymer gels.[10,16,36] Assuming affine network deformation, various entropic models derive gel elasticity from the mechanics of individual filaments comprising the gel. Another class of non-affine models account for the gel elasticity from the bending of semi-flexible or stiff filaments, and predict non-affine network deformation. Network rearrangements under external load have also been shown, both theoretically[17,40,45] and experimentally,[48] to be an additional source of non-affinity. We also discussed currently available experiments on non-affine deformations in hydrogels.

Results from various experiments show significant non-affine deformation in both (flexible) synthetic hydrogels and (semi-flexible) bio-polymer gels. The length scale of non-affine deformation, quantified from displacements of fluorescence markers, ranges from 0.1 micrometer to a few micrometers. Due to the difference in their definition of non-affinity, numbers obtained from different experimental techniques are not always directly comparable. The non-affinity in flexible PA gels is, however, measurably smaller than that in gels made of semi-flexible fibrin fibers (see Fig. 4(a)). Also, several qualitative conclusions can be drawn from the experiments. The non-affinity in semi-flexible actin networks is determined by network parameters such as crosslinker density and filament length: decreasing crosslinker density, or shortening filament length leads to higher non-affinity in actin gels.[36,51]

Non-affine deformations in polyacrylamide gels are analyzed under the lines of a recent theory of random elastic media.[22] As a flexible polymer network, the effects of filament bending that are proposed to cause non-affine deformation should be negligible in PA gels. Instead, the unexpectedly high measures of non-affinity in PA gels appear to arise from inhomogeneities that get locked into the gels during sample preparation. Such inhomogeneities have been measured using different experimental techniques like X-ray and neutron scattering. Information on the size of inhomogeneities in gels gleaned from the scattering methods, non-affinity measurements from confocal rheoscope, and theoretical studies on random elastic media, all taken together, allow us to estimate the local fluctuations in elasticity in seemingly homogeneous polymeric hydrogels like PA gels. Inhomogeneities, a major contributing factor to non-affine deformation, exist not only in synthetic polyacrylamide gels, but also in bio-polymer gels such collagen[44] and fibrin.[47]

In summary, non-affine deformation in polymeric hydrogels may be the result of such penomena as filament bending, entropic extension of worm-like chains, or network rearrangements, or even a combination of these; a picture that is further complicated by the ubiquitous presence of network inhomogeneities. Given this complexity, we believe that a more appropriate way to test the validity of the theoretical models is to characterize the deformation of individual constituent polymers as part of a globally deforming gel. It is also imperative that one accounts for static inhomogeneities and their effect on non-affinity in theoretical models, if one wishes to capture the behavior of real-world polymer gels through theoretical modeling. Lastly, non-affinity may very well be a time-dependent phenomenon. To date, most works, both theoretical and experimental, have studied the non-affinity problem from a static point of view. To gain better insight into the different relaxation mechanisms in polymer gels, it may be beneficial to explore the non-affinity question, both theoretically and experimentally, from a time-dependent perspective.

## Acknowledgements

## References

1 P. Tomasik, *Chemical and functional properties of food saccharides*, CRC Press LLC, 2003.
2 P. B. Morgana, N. Efron, M. Helland, M. Itoi, D. Jones, J. J. Nichols, E. van der Worp and C. A. Woods, *Contact Lens Anterior Eye*, 2010, **33**, 196–198.
3 H. Lodish, A. Berk, S. L. Zipursky, P. Matsudaira, D. Baltimore, J. Darnell, *Molecular Cell Biology*, 4th edition, W. H. Freeman, 2000; R. P. Mecham, *The Extracellular Matrix: An Overview*, Springer, 2011.
4 L. Dong and A. Hoffman, *J. Controlled Release*, 1991, **15**, 141–152.
5 X. S. Wu, A. S. Hoffman and P. Yager, *J. Polym. Sci., Part A: Polym. Chem.*, 1992, **30**, 2121–2129.
6 B. Kos and D. Lestan, *Plant Soil*, 2003, **253**, 403–411.
7 Y. Qiu and K. Park, *Adv. Drug Delivery Rev.*, 2001, **53**, 321–339.
8 K. S. Anseth, C. N. Bowman and L. Brannon-Peppas, *Biomaterials*, 1996, **17**, 1647–1657.
9 P. A. Janmey, E. J. Amis and J. D. Ferry, *J. Rheol.*, 1982, **26**, 599–600.
10 C. Storm, J. J. Pastore, F. C. MacKintosh, T. C. Lubensky and P. A. Janmey, *Nature*, 2005, **435**, 191–194.
11 M. L. Gardel, J. H. Shin, F. C. MacKintosh, L. Mahadevan, P. Matsudaira and D. A. Weitz, *Science*, 2004, **304**, 1301–1305.
12 M. L. Gardel, F. Nakamura, J. Hartwig, J. C. Crocker, T. P. Stossel and D. A. Weitz, *Phys. Rev. Lett.*, 2006, **96**, 088102.
13 P. A. Janmey, M. E. McCormick, S. Rammensee, J. L. Leight, P. C. Georges and F. C. MacKintosh, *Nat. Mater.*, 2007, **6**, 48–51.
14 H. Kang, Q. Wen, P. A. Janmey, J. X. Tang, E. Conti and F. C. MacKintosh, *J. Phys. Chem. B*, 2009, **113**, 3799–3805.
15 E. Conti and F. C. MacKintosh, *Phys. Rev. Lett.*, 2009, **102**, 088102.
16 F. C. MacKintosh, J. Kas and P. A. Janmey, *Phys. Rev. Lett.*, 1995, **75**, 4425–4428.
17 P. R. Onck, T. Koeman, T. van Dillen and E. van der Giessen, *Phys. Rev. Lett.*, 2005, **95**, 178102.
18 O. Lieleg, M. M. A. E. Claessens, C. Heussinger, E. Frey and A. R. Bausch, *Phys. Rev. Lett.*, 2007, **99**, 088102.
19 A. M. Stein, D. A. Vader, L. M. Jawerth, D. A. Weitz and L. M. Sander, *J. Microsc.*, 2008, **232**, 463–475.
20 A. M. Stein, D. A. Vader, L. M. Jawerth, D. A. Weitz and L. M. Sander, *Complexity*, 2011, **16**, 22–28.
21 Y. Yang, L. M. Leone and L. J. Kaufman, *Biophys. J.*, 2009, **97**, 2051–2060.
22 A. Basu, Q. Wen, X. Mao, T. C. Lubensky, P. A. Janmey and A. G. Yodh, *Macromolecules*, 2011, **44**, 1671–1679.
23 L. R. G. Treloar, *The Physics of Rubber Elasticity*, Clarendon Press, Oxford, 1975.
24 Q. Wen, A. Basu, J. P. Winer, A. Yodh and P. A Janmey, *New J. Phys.*, 2007, **9**, 438.
25 R. E. Shadwick, *J. Exp. Biol.*, 1999, **202**, 3305–3313.

26 R. H. Ewoldt, A. E. Hosoi and G. H. McKinley, *J. Rheol.*, 2008, **52**, 1427–1458.
27 C. Heussinger, B. Schaefer and E. Frey, *Phys. Rev. E: Stat., Nonlinear, Soft Matter Phys.*, 2007, **76**, 031906.
28 R. G. Larson, *The Structure and Rheology of Complex Fluids*, Oxford University Press, 1998.
29 L. A. Hough, M. F. Islam, P. A. Janmey and A. G. Yodh, *Phys. Rev. Lett.*, 2004, **93**, 168102.
30 B. R. Dasgupta and D. A. Weitz, *Phys. Rev. E: Stat., Nonlinear, Soft Matter Phys.*, 2005, **71**, 021504.
31 Paul J. Flory, *Principles of Polymer Chemistry*, Cornell University Press, 1953.
32 E. M. Huisman, Q. Wen, Y. Wang, K. Cruz, G. Kitenbergs, K. Erglis, A. Zltins, A. Cebers and P. A. Janmey, *Soft Matter*, 2011, **7**, 7257–7261.
33 J. H. Shin, M. L Gardel, L. Mahadevan, P. Matsudaira and D. A. Weitz, *Proc. Natl. Acad. Sci. U. S. A.*, 2003, **101**, 9636–9641.
34 P. J. Flory and J. Rehner, *J. Chem. Phys.*, 1943, **11**, 512–520.
35 H. M. James and E. Guth, *J. Chem. Phys.*, 1943, **11**, 455–481.
36 D. H. Head, A. J. Levine and F. C. MacKintosh, *Phys. Rev. E: Stat., Nonlinear, Soft Matter Phys.*, 2003, **68**, 016907.
37 J. Marko and E. Siggia, *Macromolecules*, 1995, **28**, 8759–8770.
38 B. A. DiDonna and T. C. Lubensky, *Phys. Rev. E: Stat., Nonlinear, Soft Matter Phys.*, 2005, **72**, 066619.
39 J. Orberg, E. Baer and A. Hiltner, *Connect. Tissue Res.*, 1983, **11**, 285–297.
40 E. M. Huisman, C. Storm and G. T. Barkema, *Phys. Rev. E: Stat., Nonlinear, Soft Matter Phys.*, 2010, **82**, 061902.
41 P. L. Chandran and V. H. Barocas, *J. Biomech. Eng.*, 2006, **128**, 259–270.
42 P. de Gennes, *Scaling Concepts in Polymer Physics*, Cornell University Press, 1979.
43 A. Hecht, R. Duplessix and E. Geissler, *Macromolecules*, 1985, **18**, 2167–2173.
44 D. G. Hepworth, A. Steven-fountain, D. M. Bruce and J. F. V. Vincent, *J. Biomech.*, 2001, **34**, 341–346.
45 M. Rubinstein and S. Panyukov, *Macromolecules*, 1997, **30**, 8036–8044.
46 A. J. Levine, D. A. Head and F. C. MacKintosh, *J. Phys.: Condens. Matter*, 2004, **16**, S2079–S2088.
47 E. A. Ryan, L. F. Mockros, J. W. Weisel and L. Lorand, *Biophys. J.*, 1999, **77**, 2813–2826.
48 T. W. Gilbert, M. S. Sacks, J. S. Grashow, S. L.-Y. Woo, S. F. Badylak and M. B. Chancellor, *J. Biomech. Eng.*, 2006, **128**, 891–898.
49 T. A. Ulrich, A. Jain, K. Tanner, J. L. MacKay and S. Kumar, *Biomaterials*, 2010, **31**, 18751884.
50 C. P. Broedersz, X. Mao, T. C. Lubensky and F. C. MacKintosh, *Nat. Phys.*, 2011, **7**, 983–988.
51 J. Liu, G. H. Koenderink, K. E. Kasza, F. C. MacKintosh and D. A. Weitz, *Phys. Rev. Lett.*, 2007, **98**, 198304.
52 S. F. Edwards and T. A. Vilgis, *Rep. Prog. Phys.*, 1988, **51**, 243–297.
53 S. F. Edwards and T. A. Vilgis, *Polymer*, 1986, **27**, 483–492.
54 C. Heussinger and E. Frey, *Phys. Rev. Lett.*, 2006, **97**, 105501.
55 E. M. Huisman and T. C. Lubensky, *Phys. Rev. Lett.*, 2011, **106**, 088301.
56 J. Wilhelm and E. Frey, *Phys. Rev. Lett.*, 2003, **91**, 108103.
57 C. P. Broedersz and F. C. MacKintosh, *Soft Matter*, 2011, **7**, 3186–3191.
58 O. Chaudhuri, S. H. Parekh and D. A. Fletcher, *Nature*, 2007, **445**, 295–298.
59 R. C. Arevalo, J. S. Urbach and D. L. Blair, *Biophys. J.*, 2010, **99**, L65–L67.
60 O. Lieleg, K. M. Schmoller, C. J. Cyron, Y. Luan, W. A. Wall and A. R. Bausch, *Soft Matter*, 2009, **5**, 1796–1803.
61 A. J. Levine and T. C. Lubensky, *Phys. Rev. E: Stat. Phys., Plasmas, Fluids, Relat. Interdiscip. Top.*, 2001, **63**, 041510.
62 M. T. Valentine, Z. E. Perlman, M. L. Gardel, J. H. Shin, P. Matsudaira, T. J. Mitchison and D. A. Weitz, *Biophys. J.*, 2004, **86**, 4004–4014.
63 K. M. Schmoller, P. Fernandez, R. C. Arevalo, D. L. Blair and A. R. Bausch, *Nat. Commun.*, 2010, **1**, 134.
64 J. M. Huyghe and C. J. M. Jongeneelen, *Biomech. Model. Mechanobiol.*, 2012, **11**, 161–170.
65 S. Badylak, K. Kokini, B. Tullius, A. Simmons-Byrd and R. Morff, *J. Surg. Res.*, 2002, **103**, 190–202.
66 S. Thomopoulos, G. M. Fomovsky, P. L. Chandran and J. W. Holmes, *J. Biomech. Eng.*, 2007, **129**, 642–650.
67 D. Vader, A. Kabla, D. Weitz and L. Mahadevan, *PLoS One*, 2009, **4**, e5902.